A Novel Approach to Enhance the Bandwidth of Miniaturized Dielectric Resonator Antennas

Amelia Buerkle*, Kamal Sarabandi, and Hossein Mosallaei
Electrical Engineering and Computer Science, The University of Michigan

Introduction and Contributions: This paper presents the concept and implementation of a wideband, high-gain miniaturized dielectric resonator antenna. A dual-resonance characteristic is achieved by merging the resonances of an aperture antenna and a dielectric resonator antenna (DRA); miniaturization is provided by the high dielectric constant of the resonator. The design enhances the bandwidth of the constituent antennas without compromising their efficiency and radiation characteristics. In addition, the design enforces low cross-polarization levels as well as a unique polarization direction over the entire bandwidth.

The technique of merging the resonance of the feed mechanism with that of the radiating structure has been employed with other types of antennas, specifically aperture-fed microstrip patch antennas [2, 3]. The benefits of DRA's over microstrip antennas which include wider bandwidth and higher efficiency encourage the extension of this principle to DRA's. Wideband DRA's have also been under development for some time; a review of many current designs may be found in [4]. These are more complex designs, however, are more difficult to fabricate, and are physically larger than the proposed method.

Theory: A diagram of the structure is shown in Fig. 1. The aperture size and position are varied in order to improve matching and control resonance frequency. As the aperture size is reduced the associated resonance moves up in frequency, occurring at approximately $\lambda_g/2$, where $\lambda_g = \lambda_o/\sqrt{\mu_{eff}\epsilon_{eff}}$ is the wavelength inside the dielectric material and μ_{eff} and ϵ_{eff} are the effective constitutive parameters seen by the aperture [6].

The fields inside the DRA may be used to relate size with operational frequency. The expressions for each field component may be obtained from the electric vector potential and the boundary conditions for the conventional dielectric waveguide model (CDWM). With reference to Fig. 1, and taking the origin at the center of the DRA, perfect magnetic walls are assumed to lie in the $x-z$ plane at $y=-b/2$ and at $y=b/2$, and in the $y-z$ plane at $x=-a/2$ and $x=a/2$. Continuity of the tangential fields is enforced at $z=h$ and, by image theory, at $z=-h$. The electric vector potential,$\vec{F}$, for the TE^z_{11} mode is then given by

$$\vec{F} = F_z\hat{z} = Acos(k_x x)cos(k_y y)sin(k_z z) \tag{1}$$

where A is a constant and the wavenumbers are as follows [8]:

$$k_x = \frac{n\pi}{b} \quad k_y = \frac{m\pi}{b} \quad k_z \tan(k_z h) = \frac{\mu_{dra}}{\mu_o}\sqrt{k_x^2 + k_y^2 - k_o^2} \tag{2}$$

where k_o is the free space wavenumber, μ_{dra} is the permeability of the DRA, and k_x,k_y,k_z are the wavenumbers in the x, y, and z directions, respectively. By replacing μ with ϵ in these equations, analogous expressions for TM modes may be found. The wavenumbers also satisfy the following characteristic equation:

$$k_x^2 + k_y^2 + k_z^2 = \mu_{r,dra}\epsilon_{r,dra}k_o^2 \tag{3}$$

where $\mu_{r,dra}$ and $\epsilon_{r,dra}$ are the relative permeability and permittivity of the DRA.

0-7803-8302-8/04/$20.00 ©2004 IEEE

The aperture can be modeled by a magnetic current source, $\vec{M} = -\hat{z} \times E_a \hat{y}$, where $E_a \hat{y}$ is the electric field in the aperture induced by currents on the ground plane. The resulting magnetic dipole current source lies along the $\hat{x}$ direction and excites the TE^x_{111} mode of the DRA. The E_z component of the TE^x_{111} mode is shown in Fig. 3(a), note the CDWM is applied and perfect magnetic walls are assumed to lie at $y = -b/2$ and $y = b/2$. Justification for the assumed PMC walls is provided in Fig. 3(b) where simulation results for the E_x and E_y components of the electric field are plotted along the x and y directions, respectively. It is observed that the normal components of the field go nearly to zero at the dielectric-air interface due to the high dielectric constant of the DRA material.

Design Analysis: Simulations are carried out using the finite-difference time-domain approach [5]. All of the simulated designs shown have dielectric resonators that are 2.67 cm square in the $x-y$ plane and 1.67 cm tall; a permittivity of 12 is used with a loss tangent of 5.6e-4. The ground plane is 5.66 cm square with a substrate thickness of 0.167 cm, $\epsilon_r = 2.2$, and $\tan\delta_e = 5.6e-4$. The microstrip feeding the aperture is 0.5 cm wide; its length varies with the design.

In Fig. 2, the variation of simulated return loss is shown as the aperture length, L_a (see Fig. 1), is varied from 3.33 cm to 2 cm while the width, w_a, is maintained at 0.5 cm. All other parameters such as resonator size and position are kept constant. The upper resonance mainly stays fixed at the same frequency while the lower resonance shifts up with decreasing aperture length. Varying aperture width also affects the lower resonance frequency and has a negligible effect on the upper resonance. These results provides evidence that the lower frequency resonance is a result of the radiation from the coupling aperture. Further simulations with DRA size confirm that the upper resonance results from the DRA.

Measured Results: An antenna similar to those simulated above is fabricated and measured. The DRA, made from TransTech's SMAT12, is 2.67 cm square by 1.67 cm tall and has $\epsilon_r = 12$ with $\tan\delta_e < 1.5e-4$. The substrate is 1.575 mm thick Rogers RT5880 ($\epsilon_r = 2.2$, $\tan\delta_e = 4-9e-4$). The antenna is on an $8cm$ square ground plane. The microstrip is $0.5cm$ wide, $L_m = 0.58cm$, and $d = 1.2mm$. The aperture dimensions are $2.1cm$ by $0.6cm$. The measured 10dB bandwidth is 29.07%. Measured and simulated return loss may be found in Fig. 4. Discrepancies between the results are primarily due to an air gap between the resonator and the ground plane. The previous equations predict a resonance frequency of 2.49 GHz, which is within 5% of the measured value of 2.57 GHz. In terms of free-space wavelength at this frequency antenna size is $0.2\lambda_o$.

Measured H-plane antenna patterns at both resonance frequencies are shown in Fig. 5. The E-plane patterns, which are not shown, exhibit asymmetry which is due, in part, to the presence of the coaxial feed to the microstrip. The H-plane patterns possess low cross-pol levels because of the similar radiation patterns of both antennas. Also, as discussed in [9] and [10], the backlobe radiation usually present with an aperture antenna is reduced by the DRA which radiates more effectively above the ground plane. The gain at the lower and upper resonant frequencies is approximately 4.6 dBi and 4 dBi, respectively.

Conclusions: It is shown that two resonances inherent to all DRA designs with resonant feed structures can be merged with proper design for bandwidth optimization. In addition, the similarity of the aperture and DRA radiation characteristics allows preservation of the radiation patterns and polarization over the entire bandwidth. The design parameters are summarized and simulation results given. A $0.2\lambda_o$ antenna exhibiting over 25% bandwidth and gain exceeding 4 dBi is built and characterized.

REFERENCES

[1] H.A.Wheeler, *Proc.IRE*, vol.35, pp.1479-1484, Dec. 1947.
[2] S. D. Targonski, R. B. Waterhouse, and D. M. Pozar, *Electron. Lett.*, vol.32, pp.1941-1942, Oct. 1996.
[3] F. Croq and A. Papiernik, *Electron. Lett.*, vol.26, pp.1293-1294, Aug. 1990.
[4] A. Petosa, A. Ittipiboon, Y. Antar, D. Roscoe, and M. Cuhaci, *IEEE Antennas Propagat. Magazine*, vol.40, pp.35-48, June 1998.
[5] H. Mosallaei, *PhD dissertation*, University of CA., Los Angeles, 2001.
[6] A. Petosa, N. Simons, R. Siushansian, A. Ittipiboon, and M. Cuhaci, *IEEE Trans. Antennas Propagat.*, vol.48, pp.738-742, May 2000.
[7] P. Sullivan and D. Schaubert, *IEEE Trans. Antennas Propagat.*, vol.34, pp.977-984, Aug. 1986.
[8] C. Balanis, *Advanced Engineering Electromagnetics*, 1989.
[9] R. Mongia and A. Ittipiboon, *IEEE Trans. Antennas Propagat.*, vol.45, pp.1348-1356, Sept. 1997.
[10] Y. Antar and Z. Fan, "*IEE Proc. Microw. Antennas Propag.*, vol.143, pp.113-118, April 1996.

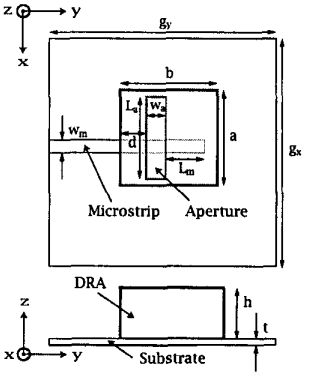

Fig. 1. Diagram of antenna design. The dielectric resonator is coupled to a microstrip-fed aperture in the ground plane.

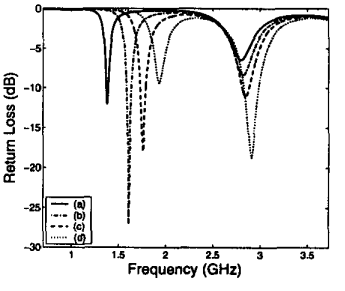

Fig. 2. The length of the aperture is varied. $w_a = 0.5cm$, $d = 1cm$,$L_m = 0.167cm$ (a) $L_a = 3.33cm$ (b) $L_a = 2.67cm$, (c) $L_a = 2.33cm$ (d) $L_a = 2cm$.

(a) E_z field component of the TE^z_{111} mode in the $y-z$ plane.

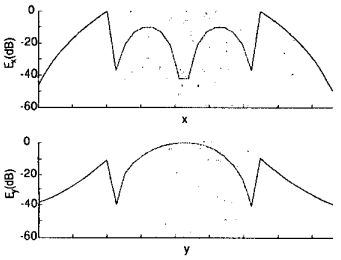

(b) E_x and E_y components inside the DRA along the x and y directions, respectively.

Fig. 3. Field patterns for the TE^z_{111} mode. (a) E_z in the $y-z$ plane. The arrows shown depict the theoretical pattern. (b) $E_x(x, y=0, z=h/2$ is given in the upper plot and $E_y(x=0, y, z=h/2$ is shown on the lower. The shaded areas represent the DRA.

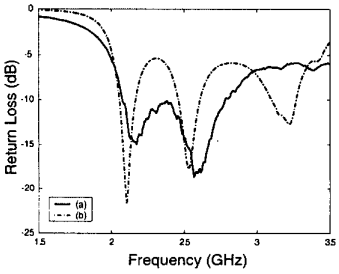

Fig. 4. Return loss for 8cm antenna design (a) measured (b) simulated.

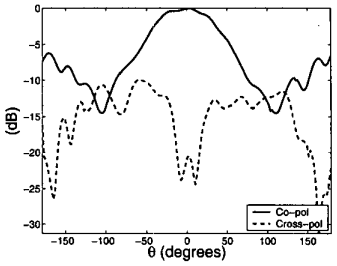

(a) Aperture Resonance $f = 2.17GHz$

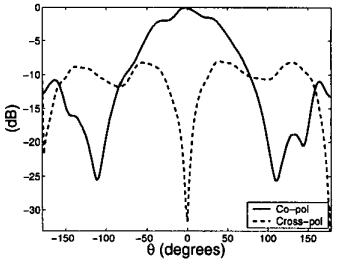

(b) DRA Resonance $f = 2.57GHz$

Fig. 5. H-plane antenna patterns for the 8cm ground plane design (a) $f = 2.17GHz$ (b) $f = 2.57GHz$